Analytical Methods

Accepted Manuscript

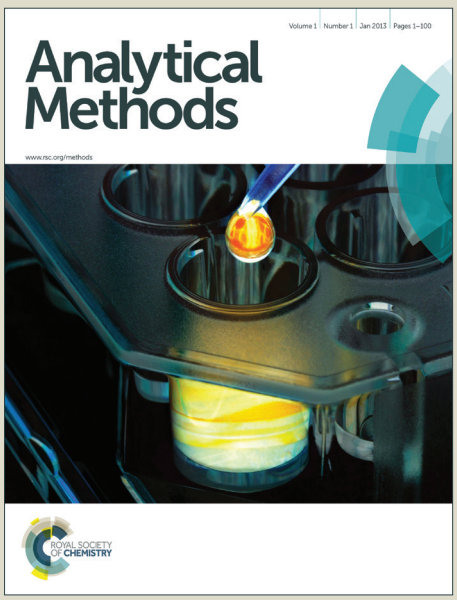

ROYAL SOCIETY OF CHEMISTRY

www.rsc.org/methods

In-situ electrochemical synthesis of Ni-capped electrochemiluminescence nanoprobe for ultrasensitive detection of cancer cells

Qingqing Wen, Pei-Hui Yang*

Department of Chemistry, Jinan University, Guangzhou 510632, China

Corresponding author:

Pei-Hui Yang, Ph.D, Professor

Department of Chemistry, Jinan University

Guangzhou 510632, China

E-mail: typh@jnu.edu.cn

Tel/Fax: +86-20-85223039

Abstract: A facile, novel and in-situ electrochemical synthesis of Ni-capped (NiS@CdS/PANINF) composite electrochemiluminescence (ECL) nanoprobe was developed to fabricate ECL cytosensor for ultrasensitive detection of cancer cells. Polyaniline nanofibers (PANINF) films were electropolymerized onto the surface of bare GCE electrode, then Ni-capped (NiS@CdS/PANINF) composite nanoprobes were successfully prepared by in-situ electrochemical approach using PANINF as template. The ECL performance of the proposed nanoprobe showed a ~5-fold enhancement compared to pure CdS NCs, which were synthesized in aqueous solution system. Further, aptamer was modified to the electrode surface to fabricate ECL cytosensor, which was identified as a recognition element of MCF-7 cancer cells. The fabricated ECL cytosensor achieved a wide dynamic range from 12 to 1.2×10^6 cells per mL for the detection of MCF-7 cancer cells, with a low detection limit of 8 cells per mL (S/N=3). This ECL cytosensor exhibited not only high sensitivity, selectivity and stability but also showed novel strategy for developing ECL biosensor system. In addition, it could be extended to highly sensitive detect other biological samples.

Key words: In-situ electrochemical synthesis; Electrochemiluminescence; NiS@CdS/PANINF composite nanoprobes; Apt; Cancer cells.

1. Introduction

Cancer is considered a worldwide mortal sickness and has become a major public concern. Identification and detection of cancer cells can provide an easy and effective way to monitor the progressions of diseases and their relevant biological processes.[1, 2] Thus, it is highly desirable to develop rapid, sensitive, and specific methods to diagnose cancers. Currently, typical methods have been applied in the field of cancer research including immunohistochemistry, polymerase chain reaction, and flow cytometry.[3-5] However, these methods suffer from false-positivity results, time-consuming, lack of efficiency and weak selectivity for the target cells.[6] To overcome this problem, some new methods or reagents are developed to detect cancer cells with high specificity and sensitivity. Aptamers are chosen as superior molecular probes for specific recognition of cancer cells, which are singe strand nucleic acid capable of binding to their target molecules.[7,8] In combination with other technical methods, some aptamer-based bioassay have been developed to detect cancer cells, such as surface acoustic wave array,[9] electrochemical methods,[10–13] surface plasmon resonance cytosensor,[14] photoluminescence,[15] due to their high affinity, specificity, ease of chemical modification, good stability, and low immunogenicity. [16] However, the sensitivity and reproducibility of these methods are weak, and it needs to be further improved.

Electrochemiluminescence (ECL) is a light emission that arises from the high-energy electron-transfer reaction between electrogenerated species at electrode surface. This technique shows potential- and spatial-controlled properties, and is highly sensitive. By integrating the interactions between biomolecules, the ECL assay has become a powerful analytical tool for highly sensitive and specific detection in biochemistry, and has been widely used in immunoassay of protein, DNA detection, carbohydrate analysis and cytosensing.[17–19] Due to the unique quantum size dependent electrochemical properties of semiconductor nanocrystals (NCs), especially II–VI NCs, which have become fascinating luminophores for the construction of biosensors.[20,21] However, NCs usually suffer from relatively weaker ECL emissions than those of conventional luminescent reagents like luminol or $Ru(bpy)_3^{2+}$. Thus, finding a way to obtain high ECL efficiency of NCs for bioanalysis is the constant driving force of this area. Many previous works have demonstrated that ECL emissions of NCs mainly occur via surface electron-hole

recombination, and are highly dependent on their surface states which can be changed by doping metal ions or composition with other nanomaterials.[22-25] It was reported that the doping of Mn^{2+} or Eu^{3+} ions in the CdS NCs surface could alter the surface of CdS NCs and create a new surface state-Mn^{2+} or Eu^{3+} complex, producing a maximum of 4-fold enhancement in ECL intensity.[26,27] Although metal ion-doped water soluble semiconductors could amplify the signal of ECL nanoprobes, they are synthesized not via in-situ system, and the process of preparing is sophisticated and time-consuming. Therefore, the development of simple, facile and in-situ synthesis is of great significance to develop the ECL system.

Electrochemical synthesis is an attractive method for the synthesis of different nanomaterials, because it is convenient, quick and parameter controllable.[28] Recently, Dhyani et al. reported the synthesis of QDs by electro-polymerization technique, which was applied to rearch the activity of enzyme based on square wave polarography.[29] Recently, Santanu have explored Ni^{2+} ion as a versatile reagent to induce both optical as well as magnetic center in various semiconductor host nanocrystals and to achieve the desired multifunctional nanocrystals.[30] Ensafi reported nickel-ferrite magnetic nanoparticles decorated with multiwall carbon nanotubes as a selective electrochemical sensor for the determination of epinephrine [31]. But their ECL performance had not been obtained, thus it provided an idea for us to in-situ synthesize based on Ni-capped ECL nanoprobe, which were expected to amplify the ECL signal of nanoprobes and improve the detection sensitivity.

Herein, a novel Ni-capped (NiS@CdS/PANINF) composite ECL nanoprobe was developed by in-situ electrochemical synthesis, which was further used to fabricate ECL cytosensor for ultrasensitive detection of cancer cells. Due to large surface area, high conductive activity, many microgaps existing between the nanofibers and positive charges on the surface, polyaniline nanofibers (PANINF) had caused widespread concern in the construction of biosensor.[32] In this work, PANINF films were electropolymerized onto the surface of bare GCE electrode, which was used as a template. Then NiS@CdS/PANINF composite nanoprobes were further formed on them by in-situ approach. Further, breast tumor cells (MCF-7 breast cancer cell line) were used as model target, on which MUC1 protein was overexpressed [33]. A 25-base oligonucleotide (Apt) with specific binding properties for MUC1 peptide was chosen to conjugate with MUC1-positive cells.[34,35] Thus, aptamer functionalized-cytosensor was fabricated to detect MCF-7 cancer cells.

This strategy of metal ions-capped nanoprobe via in-situ electrochemical synthesis had a great potential for the development of ECL system. In addition, since various recognition elements might be fused, it could be further extended to sensitive detection of other biological samples.

2. Experimental section

2.1. Materials

Nickel sulfate ($NiSO_4$), cadmium chloride ($CdCl_2$) and sodium sulfide (Na_2S) were of analytical grade and used as received. MUC1 binding aptamer: 5'-GCA GTT GAT CCT TTG GAT ACC CTG G-3' was synthesized by Shanghai Sangon Biotechnology Co. Ltd. Aniline was distilled before electro-polymerization. Phosphate buffered saline (PBS, 0.1 M pH7.4) contained 136.7mM NaCl, 2.7mM KCl, 8.72mM Na_2HPO4 and 1.41mM KH_2PO4. Millipore ultrapure water (resistivity 18.2 MΩ cm) was used throughout the experiment.

2.2. Instrumentations

The electrochemical measurements were recorded with CHI 660D electrochemical workstation (Shanghai CHI Instruments Co., China). The ECL emission measurements were conducted on a model MPI-E electrochemiluminescence analyzer (Xi'An Remax Electronic Science and Technology Co. Ltd., Xi'An, China) at room temperature, and the voltage of the PMT was set at 750 V in the process of detection. All experiments were carried out with a conventional three-electrode system. The electrochemical system consisted of a working electrode (ECL biosensor), a platinum wire as the auxiliary electrode and a reference electrode (Ag/AgCl). Scanning electron microscopic (SEM) images were obtained using a PHILIPS scanning electronmicroscope (Netherlands).

2.3. Cell lines and cell culture

Colon cancer, NPC cells and MCF-7 cancer cells were cultured in 1640 medium supplemented with 10% fetal bovine serum and with antibiotics (50UmL^{-1} penicillin, 50mg.L^{-1} streptomycin, and 10mg.L^{-1} neomycin) in an incubator (5% CO_2, 37□). Before detection, the cells were collected and separated from the medium by centrifugation at 1000rpm for 2min and then re-suspended in the PBS (0.1 M pH7.4) condition to obtain a homogeneous cell suspension.

2.4. Preparation of NiS@CdS/PANINF composite nanoprobes

The GCE was pretreated before modification by polishing its surface with aqueous slurries of alumina powders (0.3 and 0.05 μm Al_2O_3) on a polishing silk. Then it was thoroughly rinsed with water and sonicated in ethanol and ultrapure water in turn. Synthesis were carried out in two steps: firstly, the 50 μl distilled aniline, 0.5 ml 1.0 M H_2SO_4 were mixed in 9 ml double distilled water, and the solution was placed in three electrode glass cell for electrochemical treatment, a current of 120 μA had been kept constant for 300 s. Then the electrode was taken out and washed properly with distilled water. Secondly, 9 ml solution containing 0.1 M $CdCl_2$, 0.1 M Na_2S were placed into the cell, 320 μA current was done for 300 s; then 0.0562 g $NiSO_4$ was added to it, and 320 μA current was done for next 300 s. Finally, the modified electrode was rinsed thoroughly with distilled water, dried and stored at 4 °C to use.

2.5. Fabrication of the ECL cytosensor

Firstly, PANINF films were electropolymerized onto the surface of bare GCE electrode, then Ni-capped (NiS@CdS/PANINF) composite nanoprobes were further formed on them by in-situ electrochemical synthesis. Secondly, the prepared bases as matrices was dropped by 20μL 25μg/mL Apt for about 80 min to produce Apt/ NiS@CdS/PANINF attached GCE by using the reaction of the amino between Apt and PANINF under the action of glutaraldehyde, and metal ions complexation between Apt and Ni^{2+} or Cd^{2+}. Then, 1 wt % BSA solution was used to block the nonspecific binding sites for 1 h. Finally, the electrode was rinsed with PBS (0.1 M pH 7.4) solutions, dried and stored at 4 °C to use as shown in Scheme 1.

2.6. Analytical procedures

Sample solutions containing various concentrations of MCF-7 cancer cells were prepared in PBS (0.1 M pH 7.4) solutions. In a typical test, the assembled ECL cytosensor was incubated in 100 μL of sample solution for 80 min at 37 °C, followed by thoroughly washing with PBS (0.1 M pH 7.4) solutions to remove unbound MCF-7 cancer cells. Before and after the incubation, the ECL responses of the electrode were both recorded in 0.1 M PBS (pH 7.4) containing 0.1 M $K_2S_2O_8$ as coreactant. The ECL signals related to the MCF-7 cells concentrations could be measured.

3. Result and discussion

3.1. Characterization of the NiS@CdS/PANINF composite nanoprobes

HESEM technique was employed to reveal the morphology of NiS@CdS/PANINF composite nanoprobes, which were used to fabricate the surface of sensor. As shown insert in Fig. 1A, it indicated that fiber structural of PANINF films had much greater exposed surface area, which was available for loading with CdS NCs. In comparison with PANINF thins, the pure CdS NCs, which were in-situ synthesized on the PANI NF thins-modified electrode, exhibited uniform morphology with the size of 10 nm as shown in Fig. 1A. However, when Ni-capped CdS nanoprobes were also synthesized via the similar approach, the size of NiS@CdS/PANINF composite nanoprobes increased to ~50nm, because it may be that Ni^{2+} lied mostly on the surface of CdS NCs to form sulfide, and was also incorporated in CdS NCs via successively precipitation method as shown in Fig. 1B.

3.2. Electrochemical characterizations of the cytosensor

Cyclic voltammetry (CV) and electrochemical impedance spectroscopy (EIS) were used to verify the assembly processes of the modified electrodes step by step. Fig. 2A displayed the CV curves of

the modified GCE using $Fe(CN)_6^{4-/3-}$ as an electroactive probe. A couple of reversible redox peaks for the bare GCE were observed (curve a). When PANINF thins were modified onto the electrode via electro-polymerization, the peak current of the electrode increased (curve b) due to the large surface and the excellent electrical conductivity of PANINF. Then NiS@CdS/PANINF composite nanoprobes were further formed on them by in-situ electrochemical synthesis, the peak current further increased (curve c), which indicated that the proposed nanoprobes promoted the electron transfer easierly. When Apt and BSA were immobilized onto the above electrode respectively, an obvious decrease in the amperometric signal were found (curve d and e). The peak current in the CV further decreased, and the gap between the anodic and cathodic peaks became wider after subsequent specific recognition of Apt with MCF-7 cancer cells (curve f). The phenomenon resulted from the electron inert feature of Apt and MCF-7 cancer cells, which blocked the electron transfer and mass transfer of $Fe(CN)_6^{4-/3-}$ at the modified GCE surface. The EIS spectra were shown in Fig. 2B. Niquist plots comprise a semicircle part at higher frequency range and a straight linear part at lower frequency range. The diameter of the semicircle equals to the electron transfer resistance (R_{et}) at the electrode interface. Due to the good electronic transfer ability, the PANINF-modified GCE (curve b) and further proposed nanoprobes-modified electrode (curve c) exhibited lower R_{et} than bare GCE (curve a). It was clear that the diameter of the semicircles increased successively with sequential assembly of Apt (curve d), BSA (curve e) and specific recognition of MCF-7 cancer cells (curve f), indicating an enhancement of the R_{et} step by step. These results were well consistent with the phenomena in CVs, confirming the successful preparation of the cytosensor.

3.3. ECL behavior of the cytosensor

The ECL behavior of the cytosensor was investigated in 0.1 M PBS (pH 7.4) with 0.1M $K_2S_2O_8$ during the CV scanning. In Fig. 3A, it exhibited ~5-fold enhancement of the ECL intensity as compared to pure CdS NCs under the same concentration, demonstrating that Ni^{2+} was similar to Eu^{3+}. It may lie mostly on the surface of CdS NCs to form sulfide, and was also incorporated in CdS NCs via successively precipitation method to create a new surface state-Ni^{2+} complex, which accelerated the electron transfer in ECL reaction.[27,30] Fig. 3B showed the ECL emission as a

function of potential on the biosensor. The bare GCE and PANINF thins modified electrode produced a weak ECL response (curve a and b). Upon modifying NiS@CdS on the PANINF thins, a remarkable ECL increase was observed (curve c). When Apt and BSA were immobilized onto the NiS@CdS/PANINF composite nanoprobes modified electrode respectively, the ECL signal decreased apparently (curve d and e), for which they hindered the diffusion of luminescent reagents toward the electrode surface. Finally, the ECL intensity further decreased (curve f) after incubation with MCF-7 cancer cells, due to the specific recognition of Apt with MUC1. As a result, we could make a conclusion that the fabricated ECL cytosensor could be used to detect cancer cells.

3.4. ECL mechanism of NiS@CdS/ PANINF composite nanoprobes

In order to verify the ECL mechanism of NiS@CdS/PANINF, a series of experiment was implemented. As shown in Fig. 4A, PANI NF thins modified electrode produced a weak ECL response. Then PANINF thins modified electrode was placed into the solutions, which contained 0.03M Ni^{2+} and 0.1M Na_2S, the electrode also produced a weak ECL response by in-situ electrochemical synthesis. However, NiS@CdS/PANINF composite nanoprobes modified electrode produced a strong ECL response. The electrochemical behaviors of Ni^{2+} and NiS were also investigated under cyclic voltammetric scanning in the negative direction from 0 to -1.8V. The results showed PANI NF thins modified electrode produced a pair of oxidation and reduction peaks (-0.2V and -1.1V) in the solutions containing 0.03M Ni^{2+} and 0.1M Na_2S, whereas the peaks were not be observed in the solutions only containing 0.03M Ni^{2+} (Fig. 4B).

The ECL emission performance of NiS@CdS/PANINF composite nanoprobes was closely related to the stability of the reduced NiS@CdS. Fig. 4C and 4D showed the electrochemical behaviors of NiS@CdS/PANINF nanoprobes. It was clearly observed that the reduced-state NiS@CdS/PANINF nanoprobes (-1.4V) formed in the negative direction scan were so stable that they could be oxidized again (-0.8V) when scanning back without the presence of a co-reactant. For pure CdS NCs, a pair of oxidation and reduction peaks (-0.8V and -1.1V) were observed, indicating that the reduction was from the intermediate states caused by Ni^{2+} capping, and also indicating an Ni^{2+} ion–surface crystal lattice complex was formed, also the capping of Ni^{2+} into

CdS NCs made the reduced-state nanoprobes more stable. Thus, in the presence of co-reactant $K_2S_2O_8$, the ECL processes of the as-prepared NiS@CdS/PANINF composite nanoprobes were proposed as follows:[36]

$$NiS@CdS/PANINF + ne^- \rightarrow n(NiS@CdS/PANINF)^{-\bullet} \quad (1)$$

$$S_2O_8^{2-} + e^- \rightarrow SO_4^{2-} + SO_4^{-\bullet} \quad (2)$$

$$(NiS@CdS/PANINF)^{-\bullet} + SO_4^{-\bullet} \rightarrow (NiS@CdS/PANINF)^* + SO_4^{2-} \quad (3)$$

$$(NiS@CdS/PANINF)^* \rightarrow NiS@CdS/PANINF + h\upsilon \quad (4)$$

3.5. Optimization of experimental conditions

In this work, the capped metal ions may lie mostly on the surface, which made it ideal to research the Ni^{2+}-capping effect by ECL. As shown in Fig. 5A, the ECL intensity reached the maximum when the Ni^{2+}-capping concentration was 0.03M, resulting in ECL enhancement compared to pure CdS NCs. The initial increase of the ECL intensity was due to the formation of more and more Ni^{2+} luminescent centers, whereas the quenching of the ECL intensity at higher Ni^{2+}-capping level might be due to the interaction of the neighboring Ni^{2+} ions on the surface of NiS@CdS/PANINF. [37] The current and time of electrochemical synthesis condition of NiS@CdS on the PANINF thins were optimized, as shown in Fig. 5B and Fig. 5C, the ECL intensity elevated with increasing current and time, then reached the maximum. Thus, 300 μA and 300 s were selected as the optimal condition. Furthermore, the concentration of Apt, the incubation time of Apt on the surface of electrode and the time of specific recognition of Apt with MCF-7 cancer cells were related to the sensitivity of cytosensor. As shown Fig. 5D, Fig. 5E and Fig. 5F, when the concentration of Apt, the incubation time of Apt and the time of specific recognition were 25μg/mL, 80 min and 80 min, the ECL intensity achieved stable value, indicating that the interface of electrode was saturated. Thus, 25μg/mL, 80 min and 80 min were selected as the optimal condition.

3.6. Selectivity of the ECL cytosensor for MCF-7 cancer cells detection

The selectivity of ECL biosensor for MCF-7 cancer cells detection was tested via comparing the changes of ECL signal brought by other cancer cells: Colon cancer and NPC cells. In Fig. 6, the

ECL responses of cytosensor were compared after incubation with Colon cancer and NPC cells under the same experimental conditions. A slight decrease was observed in the cases of Colon cancer and NPC cells, which might be explained by the fact that both of them were MUC1 negative-expressing cancer cells. As for the mixture of MCF-7 cancer cells and Colon cancer cells, only slight increase was found in comparison with only MCF-7 cancer cells. These results suggested the good selectivity of this ECL cytosensor. Taking various kinds of aptamers for cells into account, the proposed method can be applied for the specific detection of MCF-7 cancer cells, and other kinds of cancer cells if appropriate aptamers were selected.

3.7. Analytical performance of the ECL cytosensor

The quantitative behavior of the fabricated ECL cytosensor for detection of MCF-7 cancer cells was assessed by measuring the dependence of the ECL intensity upon the concentration of cancer cells (Fig. 7). As shown in Fig. 7A, the ECL intensity decreased according with increasing concentration of cancer cells. The Δ_{ECL} was found to be logarithmically related to the concentration of MCF-7 cancer cells in the range from 12 to 1.2×10^6 cells per mL, the regression equation was $\Delta_{ECL} = 1482.3 \log C - 409.6$, with a correlation coefficient of 0.9984. Where C was the concentration of MCF-7 cancer cells, Δ_{ECL} was the relative ECL intensity calculated by $I_0 - I$, where I_0 and I were the ECL intensity without and with cancer cells, respectively (Fig. 7B). The limit of detection was calculated to be 8 cells per mL at the S/N ratio of 3. Notably, the detection limit of this proposed method was much lower than that of CdSe QDs and different lectin-based ECL methods (about $1 - 2\times10^3$ cells per mL),[38] and was also comparable to the C-dot@Ag-based nanoprobes and FA-functionalized biosensor assay (10 cells per mL) but with a more simple procedure,[39] making our strategy as an attractive alternative for highly sensitive detection of MCF-7 cancer cells.

3.8. Stability and reproducibility of the ECL cytosensor

Under the optimized conditions, strong and stable ECL signals were achieved on the NiS@CdS/PANINF composite nanoprobes modified GCE, as shown in Fig. 8A. The stability of cytosensor for MCF-7 cancer cells

was examined by measuring their ECL responses after storage in PBS (0.1 M pH 7.4) at 4 ^{0}C. After incubation with 1.2×10^3 cells per mL MCF-7 cancer cells, about 97.7% of the original ECL responses were retained after 1 week, and also about 94.6% of the initial ECL signals were noticed after 3 weeks, respectively, indicating that our proposed cytosensor was of acceptable stability. In addition, a series of six repetitive measurements of 1.2×10^3 cells per mL MCF-7 cancer cells yielded a relative standard deviation (RSD) of 5.6%, showing a good reproducibility of the ECL cytosensor.

3.9. Regeneration of ECL cytosensor

The regeneration of binding surfaces is important for reusable biosensors, but it is often difficult to achieve. Unlike most protein biosensors, the aptamer biosensors could be denatured and reused many times on the same surface of electrode, without loss of function. Dissociating reagents were used to dissociate the bounded MCF-7 cancer cells. As shown in Fig. 8B, using 30 mM EDTA as regeneration reagent gave the best result. The ECL cytosensor could be used continuously after 3 times, and the relative frequency shifts obtained were all more than 80% of the response obtained for the first cycle. The results was also obtained by other regeneration solutions, 0.2 mM glycine/HCl (pH 2.8), 1.2 mM NaOH, indicating that these reagents were not feasible perhaps due to denaturation of aptamer in these conditions.

4. Conclusions

In summary, a novel Ni-capped (NiS@CdS/PANINF) composite ECL nanoprobe was facilely prepared via in-situ electrochemical synthesis, and it was also successfully applied to highly sensitive ECL detection for MCF-7 cancer cells. Several advantages of our strategy were demonstrated: (1) NiS@CdS/PANINF composite ECL nanoprobe was synthesized by in-situ electrochemical synthesis technique, also its ECL performance showed ~5-fold enhancement compared to pure NCs, which were synthesized in aqueous solution system. (2) This technique was simple, facile and low-cost. Also it made the surface of ECL biosensor favorable simplicity and stability via in-situ synthesis method. (3) Apt functionalized-cytosensor was fabricated to ultrasensitive detect MCF-7 cancer cells with wide linear range, good reproducibility and

regeneration, acceptable precision, and a low detection limit of 8 cells per mL (S/N=3). (4) This method opened a promising path for other NCs to improve their ECL behaviors and could be further applied to develop highly sensitive ECL sensing systems.

Acknowledgment

This work was supported by the grants from National Natural Science Foundation of China (No. 21071064 and NO.21375048).

Notes and reference

1 S. Nagrath, L. V. Sequist, S. Maheswaran, D. W. Bell, D. Irimia, L. Ulkus, M. R. Smith, E. L. Kwak, S. Digumarthy, A. Muzikansky, *Nature*, 2007, **450**, 1235−1239.

2 E. I. Galanzha, E. V. Shashkov, T. Kelly, J. W. Kim, L. Yang, *Nat. Nanotechnol*., 2009, **4**, 855−860.

3 S. K. Singh, C. Hawkins, I. D. Clarke, J. A. Squire, J. Bayani, T. Hide, R. M. Henkelman, P. B. Dirks, *Nature*, 2004, **432**, 396−401.

4 D. Schamhart, J. Swinnen, K. H. Kurth, A. Westerhof, R. Kuster, H. Borchers, C. Sternberg, *Clin. Chem.*, 2003, **49**, 1458−1466.

5 J. A. Phillips, Y. Xu, Z. Xia, Z. H. Fan, W. H. Tan, *Anal. Chem*., 2009, **81**, 1033–1039.

6 C. Pan, M. Guo, Z. Nie, X. Xiao, S. Yao, *Electroanalysis*, 2009, **21**, 1321–1326.

7 M. Famulok, J. S. Hartig, G. Mayer, *Chem. Rev*., 2007, **107**, 3715–3743.

8 Y. H. Liao, R. Huang, Z. K. Ma, Y. X. Wu, X. M. Zhou, and D. Xing, *Anal. Chem*., 2014, **86**, 4596–4604.

9 K. Chang, Y. Pi, W. P. Lu, F. Wang, F. Pan, F. Li, S. R. Jia, J. F. Shi, S. L. Deng, M. Chen, *Biosens. Bioelectron*., 2014, **60**, 318–324.

10 Z. Yi, X. Y. Li, Q. Gao, L. J. Tang, X. Chu, *Analyst*, 2013, **138**, 2032–2037.

11 T. T. Zheng, J. J. Fu, L. H. Hu, F. Qiu, M. J. Hu, J. J. Zhu, Z. C. Hua, H. Wang, *Anal. Chem*., 2013, **85**, 5609−5616.

12 S. L. Xu, J. Y. Liu, T. S. Wang, H. L. Li, Y. Q. Miao, Y. Q. Liu, J. Wang, E. K. Wang, *Talanta*, 2013, **104**, 122–127.

13 K. Zhang, T. T. Tan, J. J. Fu, T. T. Zheng, J. J. Zhu. *Analyst*, 2013, **138**, 6323–6330.

14 H. X. Chen, Y. F. Hou, Z. H. Ye, H. Y. Wang, Z. M. Shen, Y. Q. Shu, *Sensor. Actuat. B-Chem*., 2014, **201**, 433–438.

15 Q. Xie, Y. Y. Tan, Q. P. Guo, K. M.Wang, B. Y. Yuan, J. Wan, X. Y. Zhao, *Anal. Methods*, 2014, **6**, 6809–6814.

16 W. Wei, D. F. Li, X. H.Pan, S. Q. Liu, *Analyst*, 2012, **137**, 2101–2106.

17 W. P. Liu, X. M. Zhou, D. Xing, *Biosens. Bioelectron*., 2014, **58**, 388–394.

18 J. Wang, W. W. Zhao, H. Zhou, *Biosens. Bioelectron*., 2013, **41**, 615–620.

19 Z. H. Chen, Y. Liu, Y. Z. Wang, X. Zhao, J. H. Li, *Anal. Chem*., 2013, **85**, 4431–4438.

20 Z. H. Chen, Y. Liu, Y. Z. Wang, X. Zhao, J. H. Li, *Anal. Chem*., 2013, **85**, 4431–4438.

21 L. L. Li, K. P. Liu, G. H. Yang, *Adv. Funct. Mater*., 2011, **21**, 869–878.

22 Y. Shan, J. J. Xu, H. Y. Chen, *Chem. Commun*., 2009, **8**, 905−907.

23 X. F. Wang, Y. Zhou, J. J. Xu, H. Y. Chen, *Adv. Funct. Mater*., 2009, **19**, 1444−1450.

24 F. Divsar, H. Ju, *Chem. Commun*., 2011, **47**, 9879-9881.

25 Y. H. Lu, W. H. Lin, C. Y. Yang, Y. H. Chiu, Y. C. Pu, M. H. Lee, Y. C. Tseng, Y. J. Hsu, *Nanoscale*, 2014, **6**, 8796–8803.

26 L. Deng, Y. Shan, J. J. Xu, H. Y. Chen, *Nanoscale*, 2012, **4**, 831–836.

27 J. Wang, Y. Shan, J. J. Xu, H. Y. Chen, *Electroanalysis*, 2013, **25**, 951–958.

28 M. Sankaran, K. Patrick, J. S. Keith, *Langmuir*, 2012, **28**, 5513–5517.

29 H. Dhyani, C. Dhand, B. D. Malhotra, P. Sen, Doi:10.4172/2155-6210.1000112.

30 J. Santanu, B. S. Bhupendra, J. Somnath, B. Riya, P. Narayan, *J. Phys. Chem. Lett*., 2012, **3**, 2535−2540.

31 Ali. A. Ensafi, F. Saeid, B. Rezaei, Ali. R. Allafchian, *Anal.Methods,* 2014, **6**, 6885−6892.

32 L. Zhang, J. H. Jiang, J. J. Luo, L. Zhang, J. Y. Cai, J. W. Teng, P. H. Yang, *Biosens. Bioelectron*., 2013, **49**, 46–52.

33 C. D. Pieve, A. C. Perkins, S. Missailidis, *Nucl. Med. Biol*., 2009, **36**, 703–710.

34 C. S. M. Ferreira, C. S. Matthews, S. Missailidis, *Tumor Biol*., 2006, **27**, 289–301.

35 P. Yin, Harry M. T. Choi, Colby R. Calvert, Niles A. Pierce, *Nature*, 2008, **451**, 318–322.

36 Y. Shan, J. J. Xu, H. Y. Chen, *Chem. Commun*., 2010, **46**, 5079−5081.

37 S. Biawas, S. Kar, S. Chaudhuri, *J. Phys. Chem. B*., 2005, **109**, 17526−17530.

38 E. Han, L. Ding, H. Z. Lian, H. X. Ju, *Chem. Commun*., 2010, **46**, 5446–5448.

39 L. Wu, J. S. Wang, J. S. Ren, W. Li, X. G. Qu, *Chem. Commun*., 2013, **49**, 5675–5677.

Scheme. 1 Schematic representation of preparation procedures of ECL cytosensor.

Fig. 1 HESEM images of (A) Pure CdS NCs which loaded in the PANI NF films. (B) NiS@CdS which loaded in the PANINF films. Insert: Image of PANINF films.

Fig. 2 CV (A) and EIS (B) curves for (a) GCE, (b) PANINF/GCE, (c) NiS@CdS/PANINF/GCE, (d) Apt/ NiS@CdS/PANINF /GCE, (e) BSA/Apt/NiS@CdS/PANINF /GCE, (f) cell/BSA/Apt/ NiS@CdS/PANINF /GCE in 0.5 M KCl solution with 5 mM $[Fe(CN)_6]^{4-/3-}$ (scan rate 100 mV/s, impedance spectral frequency $0.1-10^5$ Hz, amplitude 10 mV).

Fig. 3 (A) ECL behaviors curves for (a) CdS NCs/ PANINF/GCE, (b) NiS@CdS/PANINF/GCE; (B) ECL behaviors curves for (a) bare GCE, (b) PANINF/GCE, (c) NiS@CdS/PANINF/GCE, (d) Apt/ NiS@CdS/PANI NF /GCE, (e) BSA/Apt/ NiS@CdS/PANINF/GCE, (f) cell/BSA/Apt/ NiS@CdS/PANINF /GCE in 0.1M PBS (pH 7.4) containing 0.1 M $K_2S_2O_8$ and 0.1 M KCl.

Fig. 4 (A) ECL behaviors curves for PANINF/GCE, NiS@CdS/PANINF/GCE, NiS/ PANI NF/GCE; (B) Cyclic voltammograms of GCE modified with PANI NF in N_2-saturated 0.10 M K^+, pH 7.4 PBS containing different Ni^{2+}-capping concentration and 0.1 M Na_2S solutions; (C) Cyclic voltammograms of PANI NF/GCE and CdS/PANINF, respectively in N_2-saturated 0.10 M K^+, pH 7.4 PBS; (D) Cyclic voltammograms of NiS@CdS/PANINF nanoprobe modified electrode in 0.1 M PBS (pH 7.4) containing different Ni^{2+}-capping concentration, scanning in the negative direction from 0 to -1.80 V.

Fig. 5 (A) Effect of Ni^{2+}-capping level on the ECL intensity. Effect of the current (B) and the time (C) of electrochemical synthesis condition of NiS@CdS on the PANINF thins. Effect of the concentration of Apt (D), and the incubation time of Apt (E) on the ECL intensity. (F) Effect of the time of specific recognition of Apt with MCF-7 cancer cells on the ECL intensity.

Fig. 6 Selectivity analysis for MCF-7 cancer cells detection by monitoring the ECL intensity between two types of cancer cell lines at 1.2×10^3 cells per mL: Colon cancer cells and NPC cells, the mixed-sample contained 1.2×10^3 cells per mL MCF-7 cancer cells and Colon cancer cells, respectively.

Fig. 7 (A) ECL curves of the as-prepared electrodes tested by culturing with different concentrations of MCF-7 cancer cells suspension: (a) blank control, (b) 12, (c) 1.2×10^2, (d) 1.2×10^3, (e) 1.2×10^4, (f) 1.2×10^5, (g) 1.2×10^6 cells per mL. (B) The linear relationship between the degree of ECL intensity change and logarithm of MCF-7 cancer cells concentration, three measurements for each point.

Fig. 8 (A) ECL behaviors of NiS@CdS/PANINF in 0.10 M K^+, pH 7.4 PBS containing 0.1 M $K_2S_2O_8$ under continuous cyclic potential scan for 10 cycles from 0 to -1.8 V (vs.SCE) with a scan rate of 100 mV/s. (B) Comparison of the regeneration of aptamer biosensor by

different methods, the detection concentrations of MCF-7 cancer cells was 1.2×10^3 cells per mL. The regeneration reagents were 0.2 mM glycine/HCl (pH 2.8), 1.2 mM NaOH, 30 mM EDTA solution. The relative frequency shift (%) is the frequency shift measured relative to the response for the first measurement.

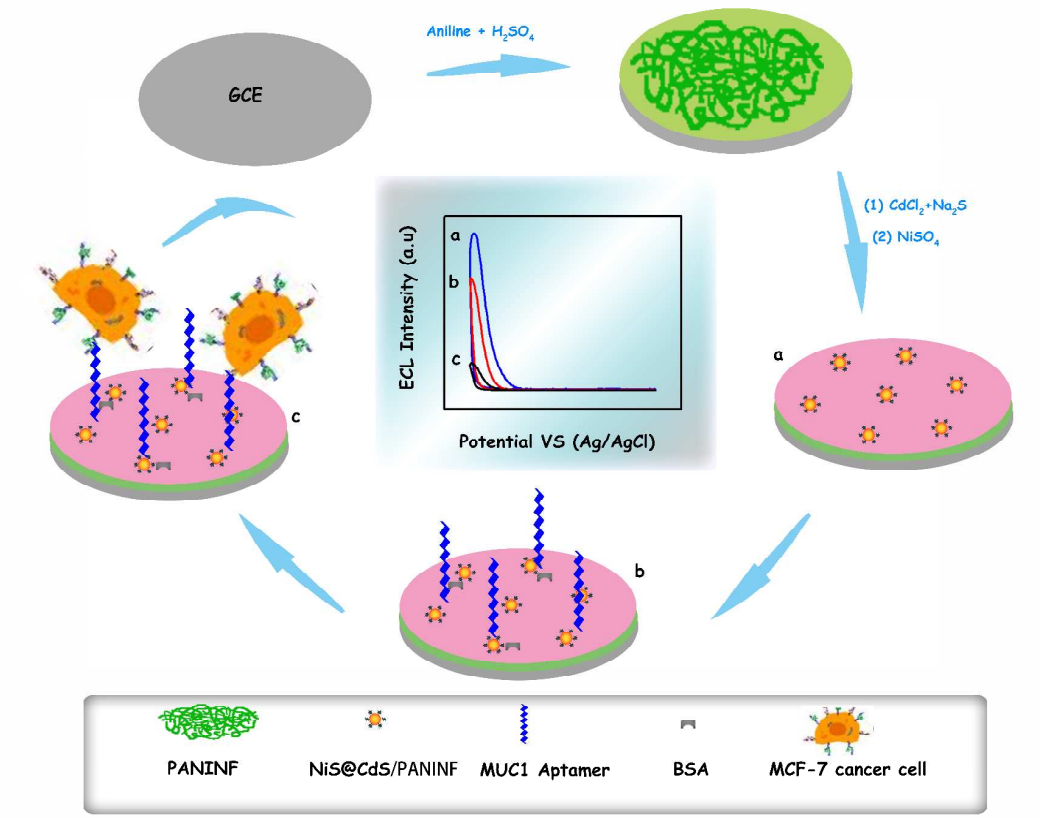

Scheme. 1

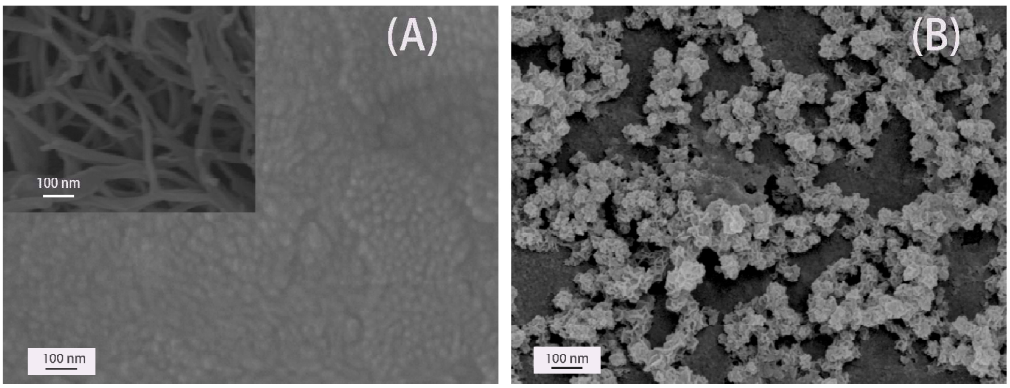

Fig. 1

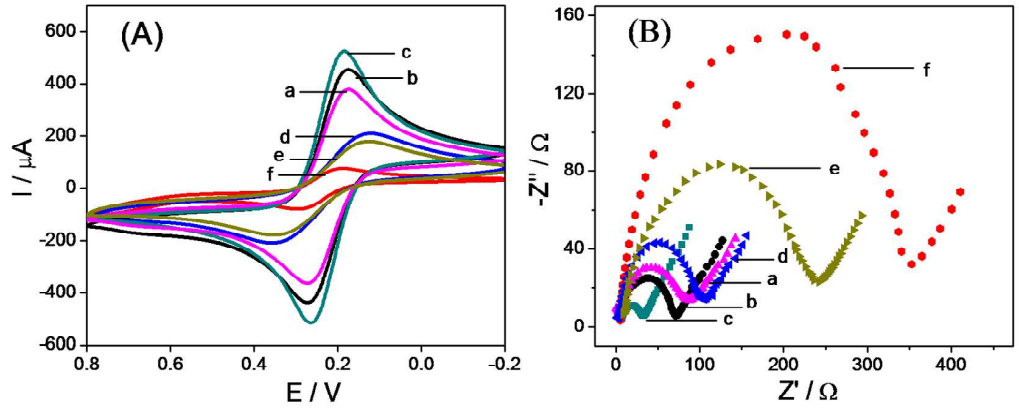

Fig. 2

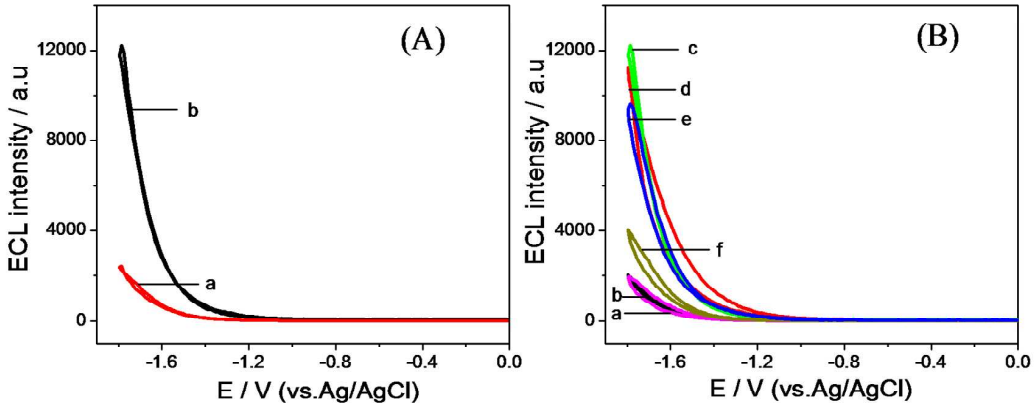

Fig. 3

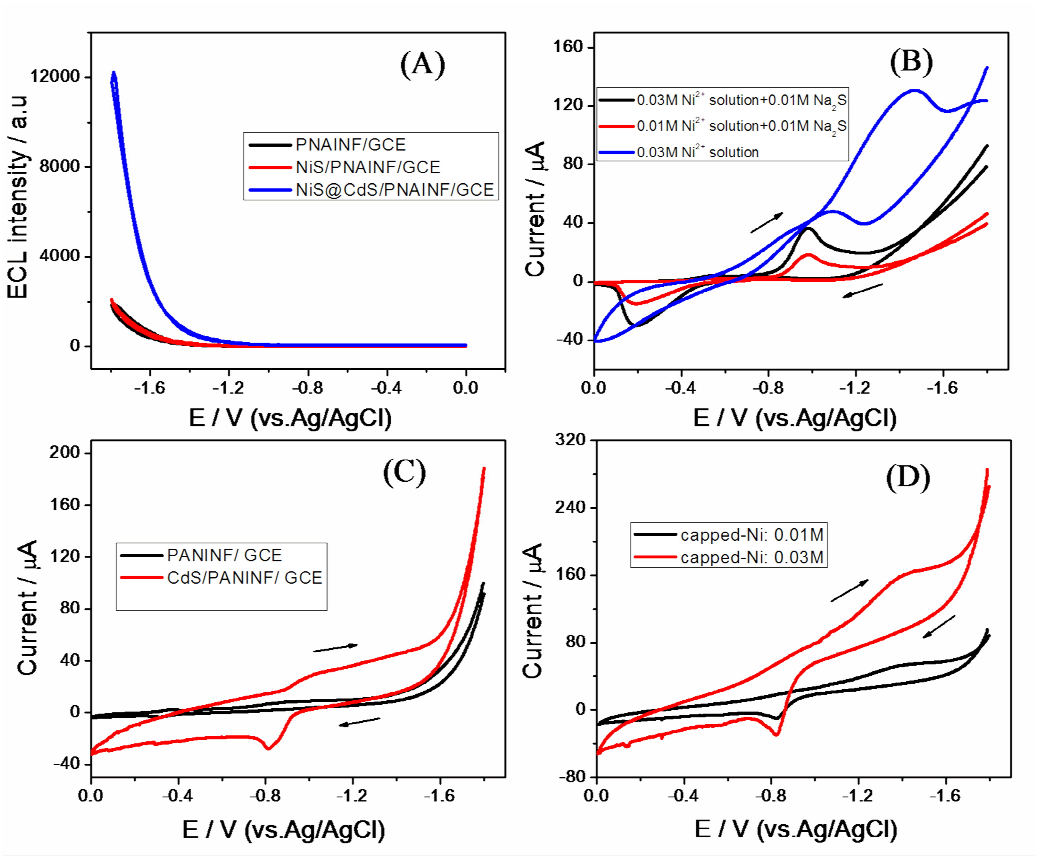

Fig. 4

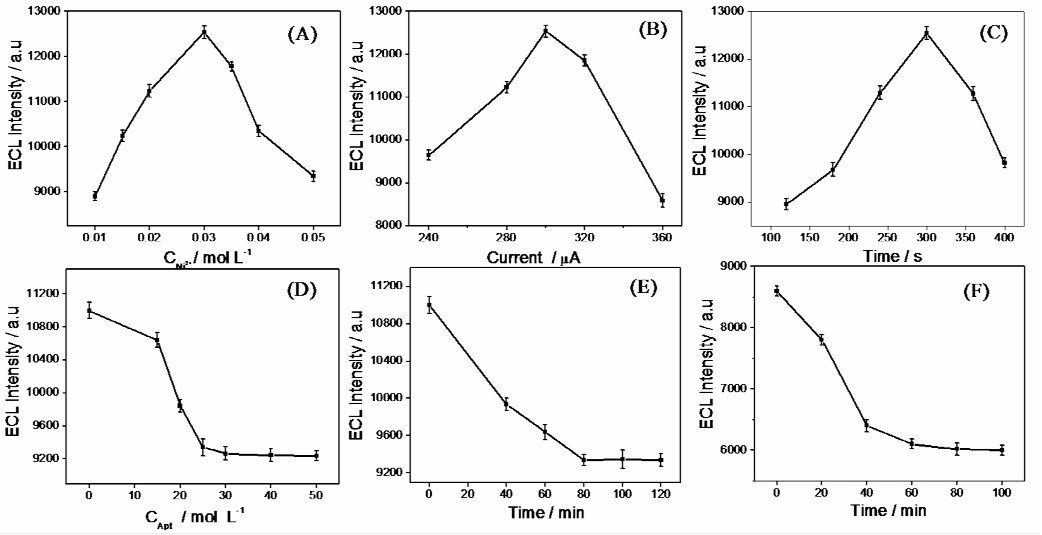

Fig. 5

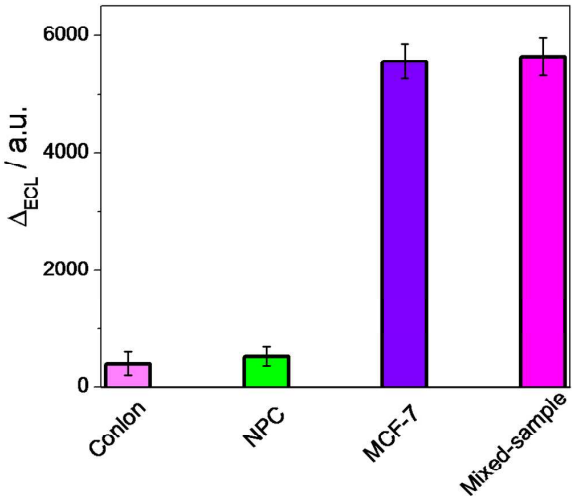

Fig. 6

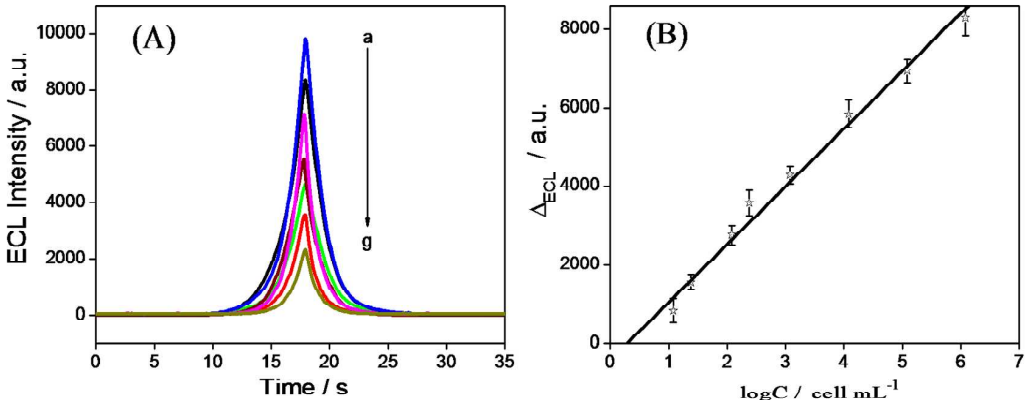

Fig. 7

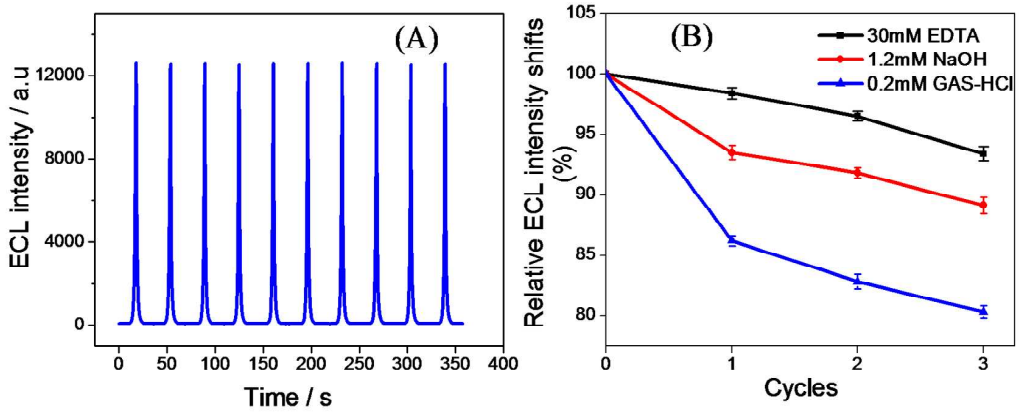

Fig. 8